ECS Transactions, 45 (3) 175-191 (2012)
10.1149/1.3700884 ©The Electrochemical Society

An Extended Unified Schottky-Poole-Frenkel Theory to Explain the Current-Voltage Characteristics of Capacitors Using High-k Dielectric Materials

W.S. Lau

Nanyang Technological University (Retired), School of EEE, Singapore 639798, Singapore

Historically, there is a controversy regarding the current-voltage (I-V) characteristics of thin film MIM (metal-insulator-metal) capacitors, which is quite frequently modeled by either the Schottky model or the Poole-Frenkel model. In this letter, the author points out that the two models actually can be unified. The physics underlying this model involves a non-uniform distribution of defect states such that a very large quantity of defect states exist at the two interface of the MIM capacitor while the density of defect states in the insulator bulk is relatively low, resulting in an M/n-i-n/M structure. This unified Schottky-Poole-Frenkel model can be further extended to include other effects like space charge limited current, tunneling, etc. Evidence supporting this theory will be provided.

Introduction

High-k dielectric materials have attracted world-wide attention for the last two decades but the current-voltage (I-V) characteristics of capacitor structures involving high-k dielectric materials is still not well understood. In the 1910's, Poole reported his experimental observations on mica insulators (1). In 1938, Frenkel followed up on Poole's work and proposed his theory that an electric field can enhance the ionization of defect states in a semiconductor (2). According to standard solid state theory, there is no basic difference between a semiconductor and an insulator except that the bandgap energy is larger for an insulator compared to a semiconductor. Hence, the Poole-Frenkel (P-F) effect can be observed in both semiconductors and insulators. For the P-F mechanism, the leakage current through an insulator is given by

$$J_{PF} = BE\exp\{[\phi_B - ((qE)/(\pi\varepsilon oK_{PF}))^{1/2}]/(kT/q)\} \quad [1]$$

In equation (1), B is a constant while E , ϕ_B , k, T, q, εo and K_{PF} are the electric field, barrier height of defect state, Boltzmann constant, absolute temperature, electronic charge, vacuum permittivity and the dielectric constant for the P-F effect.

Beside the P-F effect, leakage current can also be due to Schottky emission. For the Schottky emission mechanism, the leakage current through an insulator is given by

$$J_{SK} = A^{**}T^2\exp\{[\phi_B - ((qE)/(4\pi\varepsilon oK_{SK}))^{1/2}]/(kT/q)\} \quad [2]$$

In equation (2), A** is Richardson constant while E , ϕ_B , k, T, q, εo and K_{SK} are the

electric field, barrier height at metal-insulator interface, Boltzmann constant, absolute temperature, electronic charge, vacuum permittivity and the dielectric constant for the Schottky effect. In general, it is not easy to distinguish between the P-F mechanism and the Schottky emission mechanism because for both cases the logarithm of leakage current plotted against the square root of voltage is a straight line. In this paper, the author points out the two model can be combined into a unified Schottky-Poole-Frenkel model. In addition, this new unified Schottky-Poole-Frenkel model can be further extended to include some extra effects as explained later in this paper.

Theory

As discussed above, it is not easy to distinguish between the P-F mechanism and the Schottky emission mechanism because for both cases the logarithm of leakage current plotted against the square root of voltage is a straight line. In addition, there is also a controversy whether the dielectric constant in eq. [1] and eq. [2] is the dielectric constant at low frequency or that at optical frequency (3,4). The author would like to point out that this problem arises because equation [1] and equation [2] are used to fit the same I-V characteristics, resulting in two different values of K.; then these two different values of K will be compared with the known value of K in order to see whether equation [1] or equation [2] fits better. Then there is a controversy whether the measured value of K is the known DC dielectric constant or the dielectric constant at optical frequencies. In this paper, the author would like to point out a different approach: equation [1] and equation [2] can be used to fit two different portions of the same I-V characteristics. For example, the I-V characteristics may show a forward characteristics with current rising faster as a function of voltage compared to the reverse characteristics; then equation [1] can be used to fit the forward I-V characteristics while equation [2] can be used to fit the reverse I-V characteristics.

As discussed above, there is a controversy regarding the leakage current-voltage relationship is governed by the Schottky mechanism or by the Poole-Frenkel mechanism for several decades. The Schottky mechanism does not involve defect states in the bulk of the high-k dielectric; however, the Poole-Frenkel mechanism involves defect states in the bulk of the high-k dielectric. Previously in 2011, the author points out that these two mechanisms actually can happen simultaneously and a unified Schottky-Poole-Frenkel model can be used to explain some observed experimental data (5). The unified Schottky-Poole-Frenkel model is actually similar to a simple model involving two back-to-back Schottky diodes suggested by Lai and Lee in 1999 (6). The principal difference is the addition of a non-linear resistor RNL, which can be used to represent the Poole-Frenkel effect. In reality, the unified Schottky-Poole-Frenkel model is an extension of the model for a piece of n-type semiconductor with two metal contacts. For a capacitor structure involving a piece of n-type semiconductor with two metals, it can be represented by two back-to-back Schottky diodes with a linear resistor R separating the two Schottky diodes, as shown in Fig. 1(a). For an n-type semiconductor with shallow donors, all the donors are ionized and the current in the bulk of the semiconductor is given by

$$J = N_D q \mu_n E \qquad [3]$$

In equation [3], N_D and μ_n are the concentration of donors and electron mobility respectively. The resistance of the linear resistor R in Fig. 1(a) is given by

$$R= (N_D q \mu_n)^{-1}[(L-W_{D1}-W_{D2})/W] \quad [4]$$

In equation [4], L and W are the length and width of the piece of semiconductor respectively while W_{D1} and W_{D2} are depletion region widths of D1 and D2 in Fig. 1(a). An important assumption is that $L > W_{D1}+W_{D2}$ such that the depletion regions of D1 and D2 will not meet each other; if the depletion regions of D1 and D2 will meet each other, the linear resistor R in Fig. 1(a) will have to disappear.

According to the well-established theory of solid-state physics, an insulator is basically behaving like a semiconductor with a large bandgap. Thus it can be expected that a capacitor structure involving a piece of insulator with two metals can be represented by a model similar to that shown in Fig. 1(a). However, the linear resistor R in Fig. 1(a) has to be replaced by a non-linear resistor RNL, which can be used to represent the Poole-Frenkel effect, as shown in Fig. 1(b).

$$J_{RNL} = J_{PF} \quad [5]$$

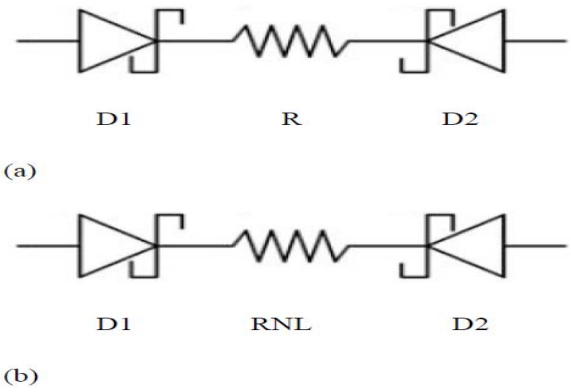

Fig. 1 (a) A capacitor structure involving a semiconductor with two metal contacts can be thought as two back-to-back Schottky diodes D1 and D2 with a linear resistor R in between. (b) A capacitor structure involving a high-k dielectric can be thought as two back-to-back Schottky diodes D1 and D2 with a non-linear resistor RNL in between. The high-k dielectric is usually a metallic oxide with oxygen vacancy type of defect states. An oxygen vacancy is a deep double donor; a high-k dielectric can be considered as a very weakly n-type large bandgap semiconductor such that D1 and D2 are drawn for metal to n-type semiconductor Schottky diodes. D1 and D2 actually represent the two interfacial regions of the capacitor and RNL represents the bulk region of the high-k dielectric.

Donors in an insulator may be deep donors. Poole-Frenkel effect is basically an electric field enhanced ionization of deep donors in an insulator. The constant B in equation [1] is proportional to the concentration of deep donors.

Lai and Lee analyzed capacitor structures involving an as-deposited tantalum oxide film which is very leaky (6); according to the model shown in Fig. 1(b), RNL is approximately zero for their work. If a high-k dielectric has oxygen vacancies, which are deep double donors, as the dominant type of donors, the high-k dielectric can be considered a very slightly n-type large bandgap semiconductor. The model shown in Fig. 1(b) is drawn assuming that the high-k dielectric behaves like a very slightly n-type large bandgap semiconductor.

There are several important assumptions in the proposed model shown in Fig. 1(b). A key assumption in the proposed model is that the dielectric constant K_{PF} for the Poole-Frenkel mechanism in eq. (1) and the dielectric constant K_{SK} for the Schottky mechanism in eq. (2) are the same. That is $K_{PF} = K_{SK}$. Another assumption is that the I-V characteristics of RNL in the proposed model is represented by eq. (1) which applies to all bias voltages and so is independent of bias voltage polarity. The last assumption is that the I-V characteristics of the Schottky diodes D1 and D2 in the proposed model is not symmetrical but instead it has a highly conductive "forward" I-V characteristics and a much less conductive "reverse" characteristics similar to the forward and reverse I-V characteristics for a metal/semiconductor Schottky diode. Eq. (2) represents the reverse characteristics of Schottky diodes D1 and D2 for relatively larger reverse bias voltages. Eq. (2) is not applicable to the forward characteristics. Furthermore, Eq. (2) may not be applicable to the reverse characteristics near zero bias voltage. Intuitively the current will be zero for zero bias voltage; however, Eq. (2) cannot produce a zero current for a zero bias voltage and thus Eq. (2) cannot be valid near zero bias voltage.

Experimental observation indicates that Poole-Fenkel effect can be observed even when the high-k insulator is a thin film with thickness smaller than 100 nm; this indicates that $L > W_{D1}+W_{D2}$ such that the depletion regions of D1 and D2 will be meet each other even when the film thickness is small. If the depletion regions of D1 and D2 meet each other, the non-linear resistor RNL in Fig. 1(b) will have to disappear. In this paper, the author attempts to propose an explanation why the depletion regions of D1 and D2 will not meet each other by proposing that there may be a very large amount of defect states at the two metal/high-k interfaces while there may be much less defect states in the bulk of the high-k dielectric as follows.

The physical basis of the model shown in Fig. 1(b) is that the native defect of high-k dielectric, which is usually a metallic oxide, is the oxygen vacancy which is a deep double donor. However, it can be easily imagined that the distribution of oxygen vacancies in the high-k dielectric is not uniform and the concentration of oxygen vacancies is largest at the two metal/high-k dielectric interfaces while there are relatively few oxygen vacancies in the bulk of the high-k dielectric. For the high-k dielectric film very close to the metal, it can be imagined that the concentration of oxygen vacancies is so big such that instead of discrete energy levels oxygen vacancies form broad bands with a shallow tail close to the bottom of the conduction band of the high-k dielectric. The bandgap of the high-k dielectric at the metal/high-k interface can be smaller than that of

the high-k dielectric in the bulk; it is very likely for the smaller bandgap interfacial material, the oxygen vacancy is a shallower donor compared to that in the bulk. In addition, according to Pearson and Bardeen, when the quantity of a deep defect state is very large, it can appear to be much shallower (7). In this way, it is very likely that the high-k dielectric behaves like an n-type large bandgap semiconductor near the top metal electrode and the bottom metal electrode. For a piece of semiconductor with metal contacts as shown in Fig. 1(a), the depletion regions of D1 and D2 will not meet each other when the n-type semiconductor near the metal/semiconductor interface has a large quantity of shallow donors. Similarly, it can be expected that for a piece of insulator with metal contacts as shown in Fig. 1(b), the depletion regions of D1 and D2 will not meet each other when the insulator near the metal/insulator interface has a large quantity of relatively shallow donor-like defect states. The author estimated that the density of the defect states at the two metal-insulator interface is probably of the order of 10^{20} to 10^{21} cm^{-3}; only when the defect state density is so high, the effect proposed by Pearson and Bardeen can be a significant effect and the depletion region thickness will be small enough. Then the capacitor structure involving high-k dielectric may look like a structure with the form of M/n-i-n/M, resulting in the model shown in Fig. 1. Previously in 1999, Hirai et al. proposed that an MIM capacitor involving a high-k dielectric can behave like an M/n^+-i-n^+/M structure (8). Subsequently in 2001, Lee et al. proposed that an MIM capacitor involving a high-k dielectric can behave like an M/n-i-n/M structure (9), which is similar to that proposed by Hirai et al. (8).

As discussed above, it can be easily imagined that when the metal is a highly reactive metal, the concentration of oxygen vacancies is largest at the two metal/high-k dielectric interfaces while there are relatively few oxygen vacancies in the bulk of the high-k dielectric. Then there is a question whether this is also the case when the metal is not highly reactive. Cho et al. pointed out that oxygen vacancies tend to segregate at the M/high-k interface (10). Tamura et al. pointed out that the formation energy of oxygen vacancies tends to become smaller at M/high-k interface even for a noble metal like Pt (11). Thus it is quite likely that even when the metal is not so highly reactive, it is still true that the concentration of oxygen vacancies is largest at the two metal/high-k dielectric interfaces while there are relatively few oxygen vacancies in the bulk of the high-k dielectric.

In a relatively old book by Shive published in 1959, the reverse I-V characteristics of a metal-semiconductor junction is controlled by the Schottky effect (12). However, subsequent study shows that the reverse I-V characteristics of a metal-semiconductor junction is complicated and the Schottky effect may be only one of many possible effects (13,14). The author would like to point out that in the absence of impact ionization (avalanche), tunneling, generation-recombination due to deep levels, the reverse I-V characteristics of a metal-semiconductor junction is probably controlled by the Schottky effect; for a metal-insulator junction, the large bandgap of the insulator probably makes impact ionization, tunneling and generation-recombination due to deep levels less likely to happen such that the reverse I-V characteristics of a metal-insulator junction is probably dominated by the Schottky effect. This is an important assumption of the theory proposed in this paper. Thus for the model shown in Fig. 1(b), the Schottky effect will be modeled by D1 (M/n) and D2 (n/M) while the Poole-Frenkel effect will be represented by the nonlinear resistance RNL ("i" in the M/n-i-n/M structure).

For a semiconductor p-n junction, the forward characteristics can be represented by a small forward voltage V_F such that the current through the p-n junction is very large when the bias voltage is above V_F while the current is zero when the bias voltage is below V_F. For a silicon p-n junction, V_F is about 0.7 V. Similarly, for a metal/semiconductor Schottky barrier, the forward I-V characteristics can be characterized by a small forward voltage V_F; V_F is usually smaller for a Schottky diode compared to a p-n junction diode. Hereby, the author proposed that: For a metal/high-k Schottky barrier, sometimes the forward I-V characteristics can also be characterized by a small forward voltage V_F. Intuitively, the forward voltage drop increases with the increase of the Schottky barrier height. Since the Schottky barrier height quite frequently increases with the work function of the metal, the author expects that the forward voltage drop increases with the work function of the metal.

The model shown in Fig. 1(b) can still be complicated and difficult to apply to a practical situation. However, the analysis of the structure shown in Fig. 1(b) can be very greatly simplified if one of the two Schottky diodes D1 and D2 has a significantly lower barrier height than the other one such that it can be considered an Ohmic contact. There can be two mechanisms. Mechanism A is a band structure effect while Mechanism B is a roughness effect, which usually happens for the bottom interface of an MIM capacitor. Firstly, the author will focus on Mechanism A: D2 has a significantly lower barrier height than D1 because of a band structure effect. According to the theoretical analysis by Robertson (15), this is the case if the metal is n^+-Si and the high-k dielectric is tantalum oxide (Ta_2O_5) or titanium oxide (TiO_2). As shown in Table I, the calculated conduction band (CB) offset on Si for Ta_2O_5 or TiO_2 is quite small and so the Schottky barrier height of n^+-Si on Ta_2O_5 or TiO_2 is quite small. As shown in Table I, the CS offset for Ta_2O_5 on Si is 0.36 eV according to theoretical calculation; experimentally, Miyazaki reported a value of 0.28 eV, which is quite close (16). Similarly, as shown in Table I, the CS offset for TiO_2 on Si is 0 eV according to theoretical calculation; experimentally, Perego et al. reported a negative value (17). As shown in Table I, the bandgap of TiO_2 is significantly smaller than that of Ta_2O_5 and CB offset on silicon is so low such that the leakage current of TiO_2 capacitors on silicon is expected to be much higher such that quite frequently Ta_2O_5 may be more suitable for microelectronics applications. Thus, in this paper, we will first concentrate on $M/Ta_2O_5/n^+$-Si capacitors where M stands for "metal". If D2 is the Schottky diode with the metal n^+-Si and the high-k dielectric Ta_2O_5, then D2 is like an Ohmic contact and so it can be ignored such that the model is Fig. 1 has only D1 and RNL left. When the metal M is positively biased, D1 is forward biased and RNL is likely to dominate over D1 such that the Poole-Frenkel mechanism dominates over the Schottky mechanism. Conversely, when the metal M is negatively biased, D1 is reverse biased and D1 is likely to dominate over RNL such that the Schottky mechanism dominates over the Poole-Frenkel mechanism. (Note: According to basic MOS theory, applying positive bias to $M/Ta_2O_5/n^+$-Si capacitors will lead to "accumulation"; applying negative bias to $M/Ta_2O_5/n^+$-Si capacitors may lead to "depletion" or "inversion", resulting in the formation of a depletion region or an inversion layer such that the model shown in Fig. 1(b) has to be modified to include the effect of a depletion region or an inversion layer. Thus, in order to see the Schottky mechanism dominating over the Poole-Frenkel mechanism when M is negatively biased, the magnitude of the negative bias voltage

cannot be too big. Alternatively, the doping concentration of the n^+-Si can be made larger such that it is not so easily depleted or inverted.) Secondly, the author will like to focus on Mechanism B: D2 has a significantly lower apparent barrier height than D1 because of the bottom interface of the MIM capacitor is significantly rougher than the top interface. This effect has been discussed by Gaillard et al. in 2006 (18). For the same applied voltage to the MIM capacitor, the electric field at the bottom interface can appear to be significantly stronger than that at the top interface. Because of the energy barrier lowering by electric field due to the Schottky effect, the barrier height at the bottom interface can become apparently lower than that at the top interface even if the bottom metal is the same as the top metal.

Table I Calculated conduction band (CB) offset on Si for Ta_2O_5 and TiO_2

Insulator	Eg (eV)	Electron affinity (eV)	Calculated CB offset on Si (eV)
SiO_2	9	0.9	3.5 (experimental)
Si_3N_4	5.3	2.1	2.4 (experimental)
Ta_2O_5	4.4	3.2	0.36
TiO_2	3.05	3.9	0

Note: The values of the experimental conduction band offset on Si for SiO_2 and Si_3N_4 are shown in Table I for the purpose of comparison. Data in Table I originate from Robertson (15).

There are three cases as follows. Case A: If the reverse biased D1 is less insulating than RNL, then the I-V characteristics follows the Poole-Frenkel theory. Let the slope of log I versus the square root of applied voltage be S_{PF}. Case B: If the reverse biased D1 is about as insulating as RNL, then the I-V characteristics is intermediate between the Poole-Frenkel theory and the Schottky theory. Then the slope of log I versus the square root of applied voltage would be between $S_{PF}/2$ and S_{PF} because of the assumption that $K_{PF} = K_{SK}$. Case C: If the reverse biased D1 is more insulating than RNL, then the I-V characteristics follows the Schottky theory. Then the slope of log I versus the square root of applied voltage would be $S_{PF}/2$ because of the assumption that $K_{PF} = K_{SK}$. In terms of physics, the slope of log I versus the square root of applied voltage would be $S_{PF}/2$ because the Schottky effect occurs at the metal/insulator interface and so is a one-sided effect while the Poole-Frenkel effects occurs in the bulk of the insulator and so is a two-sided effect; that the Schottky effect and the Poole-Frenkel effect are a one-sided effect and a two-sided effect respectively can be easily seen in Fig. 1 in ref. 3 according to Yeargan and Taylor (3).

Extended Theory

The unified Schottky-Poole-Frenkel model can be further extended to include other effects like space charge limited current by the following equation.

$$J_{RNL} = J_{PF} + J_{extra} \quad [6]$$

In the above equation, J_{PF} comes from electrons due to deep donors in the insulator. J_{extra} comes from extra electrons coming from the two metal electrodes either by thermionic emission or by quantum mechanical tunneling. It is not too difficult to imagine that for some situation there may be more electrons coming from the two metal electrodes than electrons due to deep donors in the insulator. According to space charge limited current theory, J_{extra} quite frequently followed a relationship to the bias voltage V as follows (19).

$$J_{extra} = \text{constant} \times V^{p} \quad [7]$$

In equation [7], the constant "p" can be between 2 to 5. However, the J_{extra} versus bias voltage relationship may be only piecewise continuous and may have some sudden jumps due to electron trapping as discussed by Kim et al. (19). Equation [7] only applies to the continuous regions.

For the unified Schottky-Poole-Frenkel model without this extra effect, some experimental observations cannot be explained. For example, the Schottky barrier height is low and the insulator only has a small quantity of deep donors. For the unified Schottky-Poole-Frenkel model without this extra effect, it will be expected that the I-V characteristics will show up a Poole-Frenkel type of I-V characteristics. However, experimentally, the I-V characteristics may show up a Schottky type of I-V characteristics instead. This can be explained by the extended unified Schottky-Poole-Frenkel model. There may be more electrons coming from the metal due to the small Schottky barrier height than electrons due to deep donors in the insulator such that the Poole-Frenkel effect is short-circuited, resulting in a Schottky type of I-V characteristics observed. Examples will be shown below for such a situation. For the unified Schottky-Poole-Frenkel model without this extra effect, some experimental observations showing up a space charge limited current type of I-V characteristics cannot be explained. In addition, I-V characteristics with sudden jumps cannot be explained by the basic unified Schottky-Poole-Frenkel model but by the extended unified Schottky-Poole-Frenkel model. Examples will be shown below for such a situation.

Evidence supporting Theory

Experimental evidence to support the above theory can be found in the work by Madan on a $W/Ta_2O_5/n^+$-polysilicon capacitor structure (20). Fig. 2 shows the data originally from Madan (Curve A and Curve B in Fig. 2 according to Madan) but re-plotted with the current density J in logarithmic scale versus the square root of the

magnitude of the applied voltage V. Madan did not analyze the data and now the author tries to analyze the data according to the model shown in Fig. 1 as follows. According to the above discussion, D2 in Fig. 1 can be ignored leaving only D1 and RNL because of the Mechanism A discussed above; it is also possible that the Ta_2O_5/n^+-polysilicon interface may also be rough such that Mechanism B applies. When a positive voltage is applied to the W plate, D1 is forward biased; if the forward bias voltage drop across D1 can be neglected, only RNL is left and so the I-V characteristics follows the Poole-Frenkel theory. When a negative voltage is applied to the W plate, D1 is reverse biased; if the reverse biased D1 is more insulating than RNL, then the I-V characteristics follows the Schottky theory. This can be easily seen from Fig. 2; the slope of log J vs. $V^{1/2}$ for negative voltage applied to the W plate is approximately one half of that for positive voltage applied to the W plate. The curve for positive voltage applied to the W plate can be fitted by the equation $J = 4x10^{-15}\exp(17.928V^{1/2})$ A/cm^2 while the curve for negative voltage applied to the W plate can be fitted by the equation $J = 9x10^{-13}\exp(8.562V^{1/2})$ A/cm^2; 8.562 is approximately one half of 17.928 as predicted by the author's theory. The author believes that for positive voltage applied to the W plate, the situation corresponds to case A discussed above while for negative voltage applied to the W plate, the situation corresponds to case C discussed above. Since Madan was not equipped with a suitable model, Madan could not give a proper explanation of the measured experimental data.

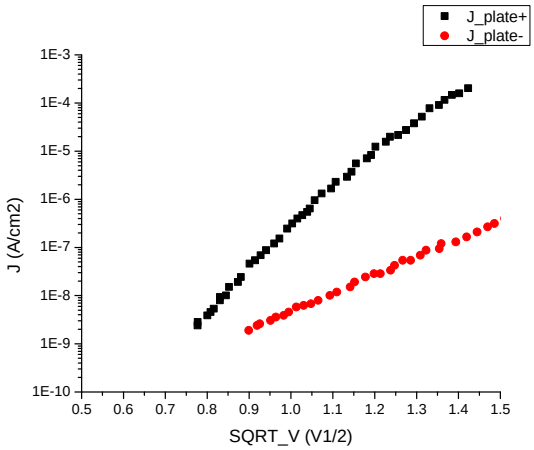

Fig. 2 Current density J plotted against the square root of voltage for a $W/Ta_2O_5/n^+$-poly-Si capacitor. The original data are from Madan 1995 (20). The physical thickness of the Ta_2O_5 film was 13.5 nm. Measurement was done at 100^{o}C. The curve for positive voltage applied to the W plate can be fitted by the equation $J = 4x10^{-15}\exp(17.928V^{1/2})$ A/cm^2 while the curve for negative voltage applied to the W plate can be fitted by the equation $J = 9x10^{-13}\exp(8.562V^{1/2})$ A/cm^2; 8.562 is approximately one half of 17.928 as predicted by the author's theory.

Experimental evidence to support the above theory can be found in the work by Kamiyama et al. on a $TiN/Ta_2O_5/W$ capacitor structure reported in 1993 (21). Kamiyama et al. pointed out that the Ta_2O_5/W interface tended to be rough in a subsequent report published in 1999 (22). It is believed the barrier height, which is a function of the metal

work function, between TiN and Ta_2O_5 and that between W and Ta_2O_5 are probably not too different; this can be seen from Table I of Matsuhashi and Nishikawa (23). Thus it is expected that the effective Schottky barrier height at the Ta_2O_5/W interface is probably significantly lower than that at the TiN/Ta_2O_5 interface by Mechanism B instead of by Mechanism A. Fig. 3 shows the data originally from Fig. 9 of Kamiyama et al. (1993) but re-plotted with the current density J in logarithmic scale versus the square root of the magnitude of the applied voltage V. According to the above discussion, D2 in Fig. 1 can be ignored leaving only D1 and RNL because of the Mechanism B discussed above. When a positive voltage is applied to the TiN plate, D1 is forward biased; if the forward bias voltage drop across D1 can be neglected, only RNL is left and so the I-V characteristics follows the Poole-Frenkel theory. When a negative voltage is applied to the W plate, D1 is reverse biased. There are two cases as follows. Case A: If the reverse biased D1 is less insulating than RNL, then the I-V characteristics follows the Poole-Frenkel theory. Case B: If the reverse biased D1 is more insulating than RNL, then the I-V characteristics follows the Schottky theory. It can be easily seen from Fig. 3 that Case A happened in the lower voltage region whereas Case B happened at the higher voltage region. In this way, the I-V characteristics is symmetrical in the lower voltage region because of the Poole-Frenkel effect. However, in the higher voltage region, the I-V characteristics follows the Poole-Frenkel theory when the voltage applied to the TiN plate is positive while the I-V characteristics follows the Schottky theory when the voltage applied to the TiN plate is negative. As shown in Fig.3, the slope of log J vs. $V^{1/2}$ for negative voltage applied to the TiN plate is approximately one half of that for positive voltage applied to the TiN plate. Since Kamiyama et al. (1993) were not equipped with a suitable model, they could not give a proper explanation of the measured experimental data.

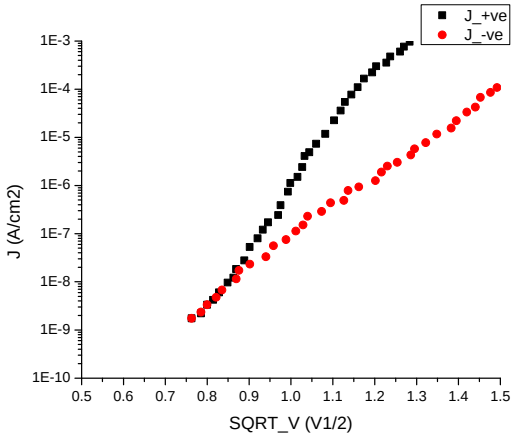

Fig. 3 Current density J plotted against the square root of voltage for a TiN/Ta_2O_5/W capacitor. The original data are from Fig. 9 in the report by Kamiyama et al. 1993 (21). The physical thickness of the Ta_2O_5 film was estimated to be about 8 nm. Electrical measurement was presumably done at room temperature.

After two examples which can be explained by the basic unified Schottky-Poole-Frenkel model, some examples which can only be explained by the extended unified Schottky-Poole-Frenkel model are given below. Fig. 4 shows the I-V characteristics of a Ta/TiO_2/n^+-Si capacitor; the original data were from Sun and Chen (24). The original plot was a semi-log plot of the current density against the electric field; Fig. 4 is a semi-log

plot of the current density against the square root of the electric field for both positive and negative voltage applied to the metal gate. It can be easily recognized that the I-V characteristics of the Ta/TiO_2/n^+-Si capacitor follow the Poole-Frenkel theory and the Schottky emission theory for positive and negative voltage applied to the metal gate, respectively. If RNL in Fig. 1(b) is totally governed by the Poole-Frenkel theory, the I-V characteristics of the Ta/TiO_2/n^+-Si capacitor should follow the Poole-Frenkel theory for both positive and negative voltage applied to the metal gate. This is because Ta is basically a low work function metal. The author would like to give an explanation according to the extended unified Schottky-Poole-Frenkel model as follows. Ta is basically a low work function metal and so the Schottky barrier height between Ta and TiO_2 is expected to be small; however, Perego et al. pointed out that the Schottky barrier height between n^+-Si and TiO_2 is negative (17). When a positive voltage was applied to the Ta gate, it is expected that electron injection from n^+-Si could be strong; however, the silicon may be oxidized during TiO_2 deposition and the silicon dioxide interfacial film may block strong electron injection from n^+-Si such that the I-V characteristics followed the Poole-Frenkel theory for positive bias applied to the Ta gate. When a negative voltage was applied to the Ta gate, electron injection from Ta could be strong such that the RNL represented by the Poole-Frenkel theory could be short-circuited by the RNL represented by space charge limited current and the I-V characteristics followed the Schottky theory for negative bias applied to the Ta gate if D1 (Ta/TiO_2 Schottky barrier) was more insulating than the RNL represented by space charge limited current.

Fig. 5 shows the I-V characteristics of a MoN/TiO_2/n^+-Si capacitor; the original data were from Sun and Chen (24). The original plot was a semi-log plot of the current density against the electric field; Fig. 5 is a semi-log plot of the current density against the square root of the electric field for both positive and negative voltage applied to the metal gate. MoN has larger work function than Ta according to Sun and Chen (24). The I-V characteristics can be explained by the extended unified Schottky-Poole-Frenkel model in a manner similar to the explanation for the I-V characteristics of a Ta/TiO_2/n^+-Si capacitor.

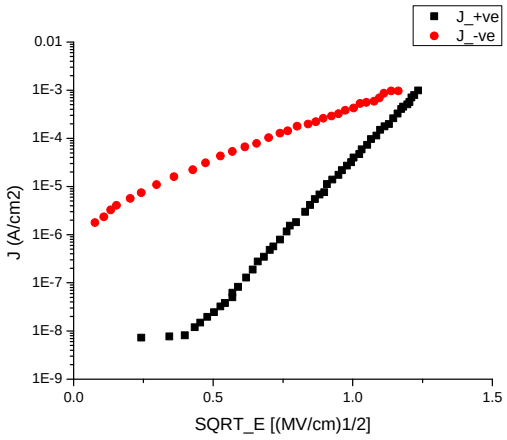

Fig. 4 A plot of the current density J against the square root of electric field for a Ta/TiO_2/n^+-Si capacitor structure for both positive and negative voltage applied to the metal gate. The slope of log J vs. $E^{1/2}$ for negative voltage applied to the Ta gate is approximately one half of that for positive voltage applied to the Ta gate.

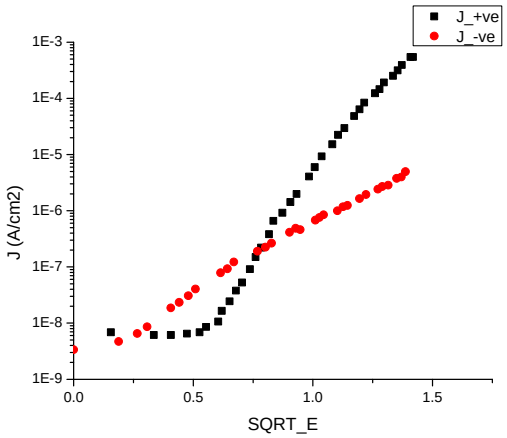

Fig. 5 A plot of the current density against the square root of electric field for a MoN /TiO_2/n^+-Si capacitor structure for both positive and negative voltage applied to the metal gate. The slope of log J vs. $E^{1/2}$ for negative voltage applied to the MoN gate is approximately one half of that for positive voltage applied to the MoN gate.

Fig. 6 shows the I-V characteristics of a Ta/TiO_2/n^+-Si capacitor and a MoN/TiO_2/n^+-Si capacitor for positive voltage applied to the metal gate. Similarly, Fig. 7 shows the I-V characteristics of a Ta/TiO_2/n^+-Si capacitor and a MoN/TiO_2/n^+-Si capacitor for negative voltage applied to the metal gate. It can be easily recognized that the I-V characteristics of a Ta/TiO_2/n^+-Si capacitor and a MoN/TiO_2/n^+-Si capacitor for positive voltage applied to the metal gate followed the Poole-Frenkel theory because the current increases faster with increase of electric field for positive bias than for negative bias and the current is less sensitive to change of the metal gate for positive bias than for negative bias. However, there was still a small shift due to the difference of the forward voltage drop (V_F) of the Ta/TiO_2 Schottky barrier and the MoN/TiO_2 Schottky barrier.

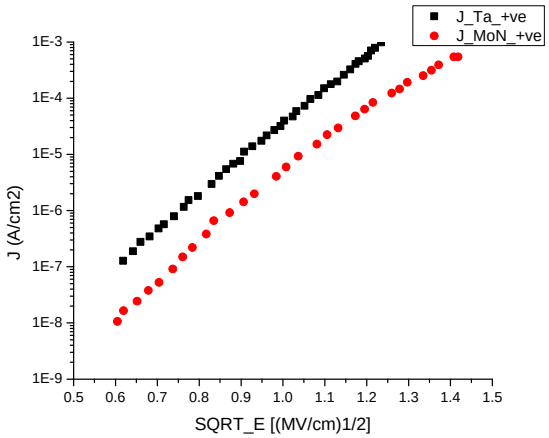

Fig. 6 A plot of the current density against the square root of electric field for Ta/TiO_2/n^+-Si and MoN/TiO_2/n^+-Si capacitor structures for positive voltage applied to the metal gate.

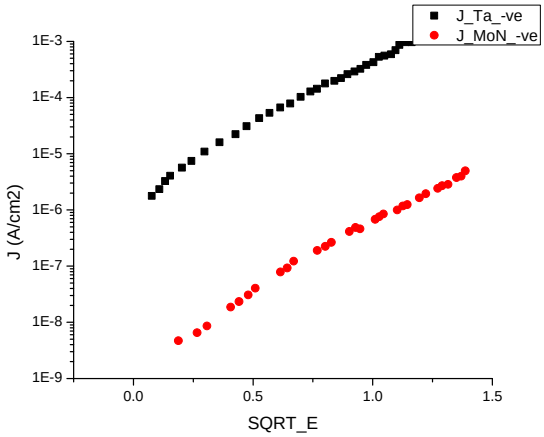

Fig. 7 A plot of the current density against the square root of electric field for $Ta/TiO_2/n^+$-Si and $MoN/TiO_2/n^+$-Si capacitor structures for negative voltage applied to the metal gate.

Similarly, it can be easily recognized that the I-V characteristics of a $Ta/TiO_2/n^+$-Si capacitor and a $MoN/TiO_2/n^+$-Si capacitor for negative voltage applied to the metal gate followed the Schottky theory; however, there was a large shift due to the difference of the effective barrier height of the Ta/TiO_2 Schottky barrier and the MoN/TiO_2 Schottky barrier.

For the unified Schottky-Poole-Frenkel model without the above mentioned extra effect, another important class of I-V characteristics which cannot be explained properly is the class of I-V characteristics with sharp jumps in the leakage current at some voltages. The author tries to re-interpret some experimental results reported by Aoyama et al. in 1996 on $TiN/Ta_2O_5/SiON/n^+$-polysilicon capacitor structures (25). As shown in Fig. 8, there is a sharp jump in the I-V characteristics when the TiN gate was biased positively. The author's explanation is that there is a large Schottky barrier height at the TiN/Ta_2O_5 interface while there is a small Schottky barrier height at the Ta_2O_5/n+-polysilicon interface. When the $TiN/Ta_2O_5/SiON/n^+$-polysilicon capacitor structure is biased negatively, the I-V characteristics can be explained by the unified Schottky-Poole-Frenkel model without the above mentioned extra effect. When the $TiN/Ta_2O_5/SiON/n^+$-polysilicon capacitor structure is biased positively, the I-V characteristics cannot be explained by the unified Schottky-Poole-Frenkel model without the above mentioned extra effect. An extended unified Schottky-Poole-Frenkel model has to be used. When the TiN gate is positively biased, electrons are injected by the n+-polysilicon into the Ta_2O_5 high-k dielectric. However, this effect is delayed by the presence of a large quantity of electron traps in the SiON layer such that the leakage current is smaller for TiN gate positively biased than for TiN gate negatively biased. When the bias voltage is increased beyond a certain "trap fill limit", the leakage current suddenly jumps up very rapidly for TiN gate positively biased and the leakage current is very strongly larger for TiN gate positively biased than for TiN gate negatively biased. Thus the fundamental reason that the leakage current is very much larger for TiN gate positively biased than for TiN gate negatively biased is that the effective Schottky barrier height of the Ta_2O_5/n^+-polysilicon interface is much smaller than that of the TiN/Ta_2O_5 interface. Furthermore, the

fundamental reason that the leakage current is smaller for TiN gate positively biased than for TiN gate negatively biased is that there is an asymmetry in the location of electron traps such that the electron traps are mainly located near the Ta_2O_5/SiON/n^+-polysilicon interface. The author believes in ultra-thin Ta_2O_5 deposited by CVD and then properly annealed there are not too many defect states in terms of deep donors and electron traps present.

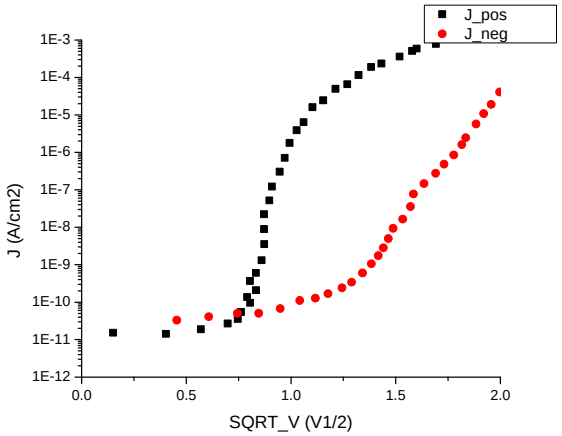

Fig. 8 Current density plotted against the square root of voltage for a TiN/Ta_2O_5/SiON/n^+-polysilicon capacitor with 650°C annealing after Ta_2O_5 deposition. The original data are from Aoyama et al. 1996 (25).

In addition, there are also I-V characteristics with sudden jumps reported for La_2O_3 capacitor structures by Kim et al. (19). The extended unified Schottky-Poole-Frenkel model is necessary to explain that category of I-V characteristics.

Further Extension of Theory Possible

Most of the discussion in this article has been concentrated on titanium oxide and tantalum oxide with a bandgap of 3.05 eV and 4.4 eV, respectively. For extension to high-k dielectric materials with larger bandgap like aluminum oxide, which has a bandgap of 8.8 eV, modification of the above model is quite frequently necessary. D1 and D2 in Fig. 1(b) may have large Schottky barrier heights such that at room temperature electrons can more easily tunnel through the energy barrier than go over the energy barrier by thermionic emission. For such a situation, equation [2] can be replaced by an equation for tunneling. Then part of the I-V characteristics may be dominated by tunneling while another part may be dominated by Poole-Frenkel model.

The Schottky barrier height is a function of the metal work function; usually when the metal work function increases, the Schottky barrier height tends to increase. However, there is another important factor; the Schottky barrier height can be significantly modified due to the presence of defect states at the metal/high-k interface. The author believes that the Schottky barrier height at the metal/high-k interface tends to become smaller when there are a lot of defect states at the metal/high-k interface. Conversely, the Schottky barrier height at the metal/high-k interface tends to become larger when the

defect states at the metal/high-k interface are reduced. For example, Schaeffer et al. reported that the effective work function of platinum on hafnium oxide becomes larger when the amount of oxygen vacancies becomes less (26); larger effective work function implies larger Schottky barrier height. In addition, the author believes that the amount of defect states at the interface tend to become larger when there is a large amount of defect states in the bulk. Thus it is not surprising that the Schottky barrier height for poorly prepared aluminum oxide capacitors with a lot of defect states tend to be smaller such that the unified Schottky-Poole-Frenkel model can be used without adding the effect of tunneling. Using low work function metal electrodes further makes the Schottky barrier height smaller. With the help of the above theory, a lot of apparent contradictions reported in the literature can be understood. In 1970, Goodman estimated that the Schottky barrier height between Al (a low work function metal with a work function of about 4.28 eV) and Al_2O_3 is about 2 eV (27). However, in 1971, Antula estimated that the Schottky barrier height between Al and Al_2O_3 is about 0.8 eV (28). The author believes that the apparent contradiction between Goodman and Antula is because the sample preparation method of Antula may not be strong enough to oxidize the aluminum oxide thin film sufficiently such that there may be much more defect states in Antula's sample compared to Goodman's sample, resulting in smaller effective energy barrier height for Antula's sample than Goodman's sample. For poorly prepared aluminum oxide capacitors using low work function metal electrodes, it is quite likely that the Schottky effect dominates over the tunneling effect at room temperature. For state-of-the-art aluminum oxide capacitors using large work function metal electrodes, it is quite likely that tunneling dominates over the Schottky effect at room temperature. For higher temperatures, the Schottky effect can dominate over tunneling. Thus it is not surprising that in 1971 Antula reported that the leakage current of aluminum oxide capacitor followed the Schottky mechanism or the Poole-Frenkel mechanism (28) whereas, in 2011, Jinesh et al. reported that the leakage current of aluminum oxide capacitor followed the tunneling mechanism or the Poole-Frenkel mechanism (29). All of these apparent contradictions can be understood by the author's explanation that better prepared samples tend to have larger effective Schottky barrier height such that tunneling tends to dominate over thermionic emission at room temperature, whereas poorly prepared samples tend to have smaller effective Schottky barrier height such that thermionic emission tends to dominate over tunneling at room temperature.

Another situation is when the high-k insulator film is relatively thick and has a relatively small bandgap and there is a very thin low-k large bandgap insulator film at the high-k insulator/metal interface; for example, there is quite frequently a very thin low-k large bandgap insulator film like SiO_x ($1<x<2$) at a high-k insulator and Si interface. One of the two Schottky diodes D1 and D2 can be replaced by a tunneling MIS diode like that in references G1 and G2. Part of the I-V characteristics of this tunneling MIS diode can be dominated by the tunneling process (30-32); electrons contributed by tunneling can be more than electrons from deep donors in the insulator. Furthermore, sometimes the high-k insulator is so thin that direct tunneling is possible; a non-linear resistor shunting across D1, RNL and D2 can be added.

Conclusion

In conclusion, the author proposed a model which unifies the Poole-Frenkel theory and the Schottky theory. In this model, the Poole-Frenkel effect and the Schottky

effect happen simultaneously but sometimes the Poole-Frenkel effect dominates over the Schottky effect and vice versa. The basic unified Schottky-Poole-Frenkel model can be used to explain quite a lot of experimental observations. For this model, the leakage current will be influenced by the defect states in the bulk of the high-k insulator. In addition, the leakage current will be influenced by the choice of metal electrodes and also by the defect states at the interfaces. However, the basic unified Schottky-Poole-Frenkel model is not sufficient for some situation. That is why an extended unified Schottky-Poole-Frenkel model is sometimes required. The extended unified Schottky-Poole-Frenkel model allows for the effect of carrier injection from the metal electrodes into the high-k insulator. When the Schottky barrier is large, especially for large bandgap high-k dielectric, the model has to be further extended to include the effect of tunneling.

Acknowledgments

The author would like to acknowledge the help of his previous graduate students and colleagues. In addition, he would like to acknowledge the support of Dr. Taejoon Han and Mr. Neal Sandler when they worked on tantalum oxide in Lam Research Corporation.

References

1. H.H. Poole, *Philosophical Magazine*, **32**, 112 (1916).
2. J. Frenkel, *Phys. Rev.*, **54**, 647 (1938).
3. J.R. Yeargan and H.R. Taylor, *J. Appl. Phys.*, **39**, 5600 (1968).
4. D.S. Jeong, H.B. Park and C.S. Hwang, *Appl. Phys. Lett.*, **86**, 072903 (2005).
5. W.S. Lau, *ECS Transactions*, **35** (4), 873-887 (2011).
6. B.C. Lai and J. Y. Lee, *J. Electrochem. Soc.*, **146**, 266 (1999).
7. G.L. Pearson and J. Bardeen, *Phys. Rev.*, **75**, 865 (1949).
8. T. Hirai, H. Morita and M. Tasaka, *Jpn. J. Appl. Phys.*, **38**, 6549 (1999).
9. M.J. Lee, K.S. Chung, J.I. Han, W.K. Kim, S.J. Hong and S.K. Park, *Journal of the Korean Physical Society*, **39**, 686 (2001).
10. E. Cho, B. Lee, C.-K. Lee, S. Han, S.H. Jeon, B.H. Park and Y.-S. Kim, *Appl. Phys. Lett.*, **92** , 233118 (2008).
11. T. Tamura, S. Ishibashi, K. Terakura and H. Weng, *Phys. Rev. B*, **80**, 195302 (2009).
12. J.N. Shive, "The Properties, Physics and Design of Semiconductor Devices", D. Van Nostrand Company, Inc., Princeton, New Jersey, USA, 1959, Chapter 20 "Theory of Metal-Semiconductor Contacts", p. 363.
13. J.M. Andrews and M.P. Lepselter, *Solid-State Electron.*, **13**, 1011 (1970).
14. E. Pascual, R. Rengel and M.J. Martin, *Semicond. Sci. Technol.*, **22**, 1003 (2007).
15. J. Robertson, *J. Vac. Sci. Technol. B*, **18**, 1785 (2000).
16. S. Miyazaki, *J. Vac. Sci. Technol. B*, **19**, 2212 (2001).
17. M. Perego, G. Seguini, G. Scarel, M. Fanciulli and F. Wallrapp, *J. Appl. Phys.*, **103**, 043509 (2008).
18. N. Gaillard, L. Pinzelli, M. Gros-Jean and A. Bsiesy, *Appl. Phys. Lett.*, **89**, 133506 (2006).
19. Y. Kim, S. Ohmi, K. Tsutsui and H. Iwai, *Jpn. J. Appl. Phys.*, **44**, 4032 (2005).
20. S.K. Madan, *IEEE Trans. Electron Dev.*, **42**, 1871 (1995).

21. S. Kamiyama, H. Suzuki, H. Watanabe, A. Sakai, M. Oshida, T. Tatsumi, T. Tanigawa, N. Kasai and A. Ishitani, IEDM Tech. Dig., p. 49 (1993).
22. S. Kamiyama, J.M. Drynan, Y. Takaishi and K. Koyama, Symp. VLSI Tech., p. 39 (1999).
23. H. Matsuhashi and S. Nishikawa, *Jpn. J. Appl. Phys.*, **33**, 1293 (1994).
24. S.C. Sun and T.F. Chen, *Jpn. J. Appl. Phys.*, **36**, 1346 (1997).
25. T. Aoyama, S. Saida, Y. Okayama, M. Fujisaki, K. Imai and T. Arikado, *J. Electrochem. Soc.*, **143**, 977 (1996).
26. J.K. Schaeffer, L.R.C. Fonseca, S.B. Samavedam, Y. Liang, P.J. Tobin and B.E. White, *Appl. Phys. Lett.*, **85**, 1826 (2004).
27. A.M. Goodman, *J. Appl. Phys.*, **41**, 2176 (1970).
28. J. Antula, *J. Appl. Phys.*, **42**, 2081 (1971).
29. K.B. Jinesh, J.L. van Hemmen, M.C.M. van de Sanden, F. Roozeboom, J.H. Klootwijk, W.F.A. Besling and W.M.M. Kessels, *J. Electrochem. Soc.*, **158**, G21 (2011).
30. M.A. Green, F.D. King and J. Shewchun, *Solid-State Electron.*, **17**, 551 (1974).
31. J. Shewchun, M.A. Green and F.D. King, *Solid-State Electron.*, **17**, 563 (1974).
32. J. Racko, P. Valent, P. Benko, D. Donoval, L. Harmatha, P. Pintes and J. Breza, *Solid-State Electron.*, **52**, 1755 (2008).